Electronic Supplementary Material (ESI) for Polymer Chemistry.

Insights into the interaction between bis(aryloxide)alkylaluminum and *N*-heterocyclic carbene: from abnormal Lewis adduct to Frustrated Lewis pair efficient polymerizations of biomass-derived acrylic monomers

Xing Wang,[b] Yanping Zhang,[b] and Miao Hong[a,b,*]

[a] *School of Chemistry and Material Sciences, Hangzhou Institute for Advanced Study, University of Chinese Academy of Sciences, 1 Sub-lane Xiangshan, Hangzhou 310024, China*

[b] *State Key Laboratory of Organometallic Chemistry, Shanghai Institute of Organic Chemistry, Chinese Academy of Sciences, Shanghai 200032, China*

[*]Correspondence to: miaohong@sioc.ac.cn

Materials, Reagents, and Methods.

All synthesis and manipulations of air- and moisture-sensitive materials were carried out in flamed Schlenk-type glassware on a dual-manifold Schlenk line or in an argon-filled glovebox. HPLC-grade organic solvents, including toluene, *n*-hexane, and dichloromethane were purified with an MBraun solvent purification system. Methyl crotonate (MC) and (*E*,*E*)-methyl sorbate (MS) were purchased from Energy Chemical Co and TCI Chemical Co. All the monomers were first degassed and dried over CaH_2 for 3 days, followed by vacuum distillation. Further purification involved titration with tri(*n*-octyl) aluminum (Sigma-Aldrich Co) to a yellow end point, followed by distillation under reduced pressure. All the purified monomers were stored in the brown bottles inside a glovebox freezer at –30 °C. 1,3-di-*tert*-butylimidazolin-2-ylidene (I^tBu) was purchased from TCI Chemical Co, and used as received. Literature procedures were employed to prepare *β*-angelica lactone (*β*-AL),[1] 1,3-diisopropyl-imidazolin-2-ylidene (I^iPr),[2] 1-(*tert*-butyl)-3-(*iso*-propyl)-imidazolin-2-ylidene (I^tBu^iPr),[3] 1-(*tert*-butyl)-3-methyl-imidazolin-2-ylidene (I^tBuMe),[4] 1,3-di-*tert*-butyl-4,5-dimethylimidazol-2-ylidene (Me-I^tBu),[5] $MeAl(BHT)_2$,[6] $EtAl(BHT)_2$,[6] $^iBuAl(BHT)_2$.[6]

Stoichiometric Reaction of Lewis Acid (LA) and Lewis Base (LB) to Form Abnormal Lewis Adducts (ALA), Classical Lewis Adducts (CLA), and Frustrated Lewis Pair (FLP)

In a typical procedure, a Teflon-valve-sealed J. Young-type NMR tube was charged with LA (0.08 mmol) in the glovebox. A solution of LB (0.08 mmol) in 0.50 mL of benzene-d_6 was added to the above NMR tube *via* pipette at RT, and the resulting mixture was then taken out of the glovebox for NMR analysis.

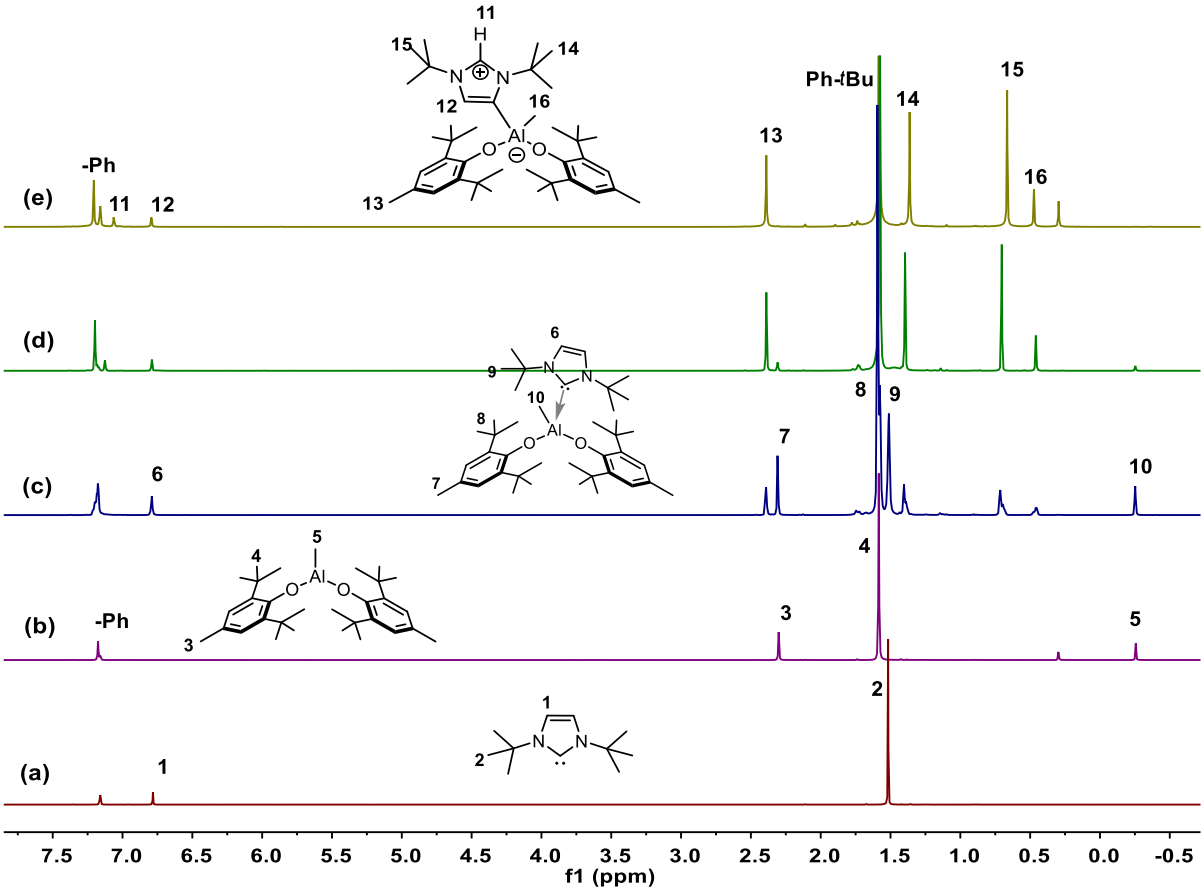

Figure S1. Monitoring of the stoichiometric reaction of I^{t}Bu and MeAl(BHT)$_2$ by ^{1}H NMR spectra (benzene-d_6, RT): (a) I^{t}Bu; (b) MeAl(BHT)$_2$; (c) 0.5 h: MeAl(BHT)$_2$/I^{t}Bu FLP (61.5%) and **ALA-1** (38.5%); (d) 3 h, FLP (13.0%) and **ALA-1** (87.0%); (e) 5 h: **ALA-1** (100.0%).

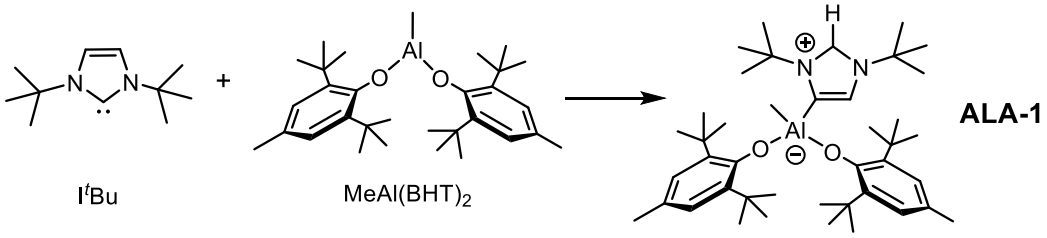

ALA-1: ^{1}H NMR (400 MHz, benzene-d_6, RT): δ 7.17 (s, 4H, Ar–*H*), 7.14 (s, 1H, –C$^+$*H*), 6.77 (s, 1H, N–C*H*=), 2.37 (s, 6H, Ar–C*H*$_3$), 1.55 (s, 36H, Ar–C(C*H*$_3$)$_3$), 1.40 and 0.71 (s, 18H, N–C(C*H*$_3$)$_3$), 0.43 (s, 3H, Al–C*H*$_3$). ^{13}C NMR (100 MHz, benzene-d_6, RT): δ 158.6, 138.9, 125.9, 123.8 (aromatic ring), 151.1 (Al–*C*=), 130.3 (N–*C*H=), 126.7 (–*C*$^+$), 59.3 and 56.9 (N–*C*(CH$_3$)$_3$), 35.6 (Ar–*C*(CH$_3$)$_3$), 32.2 (Ar–C(*C*H$_3$)$_3$), 30.8 and 29.0 (N–C(*C*H$_3$)$_3$), 21.4 (Ar–*C*H$_3$), 2.5 (Al–*C*H$_3$).

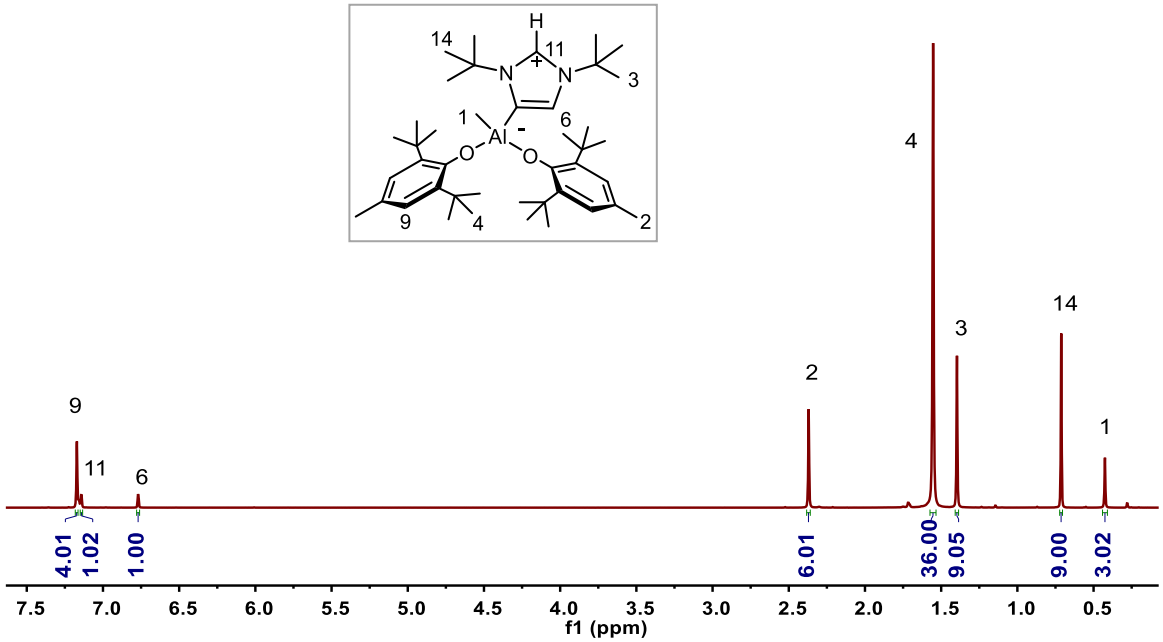

Figure S2. ^{1}H NMR spectrum of the **ALA-1** formed by the stoichiometric reaction of I^{t}Bu and MeAl(BHT)$_2$ (benzene-d_6, RT).

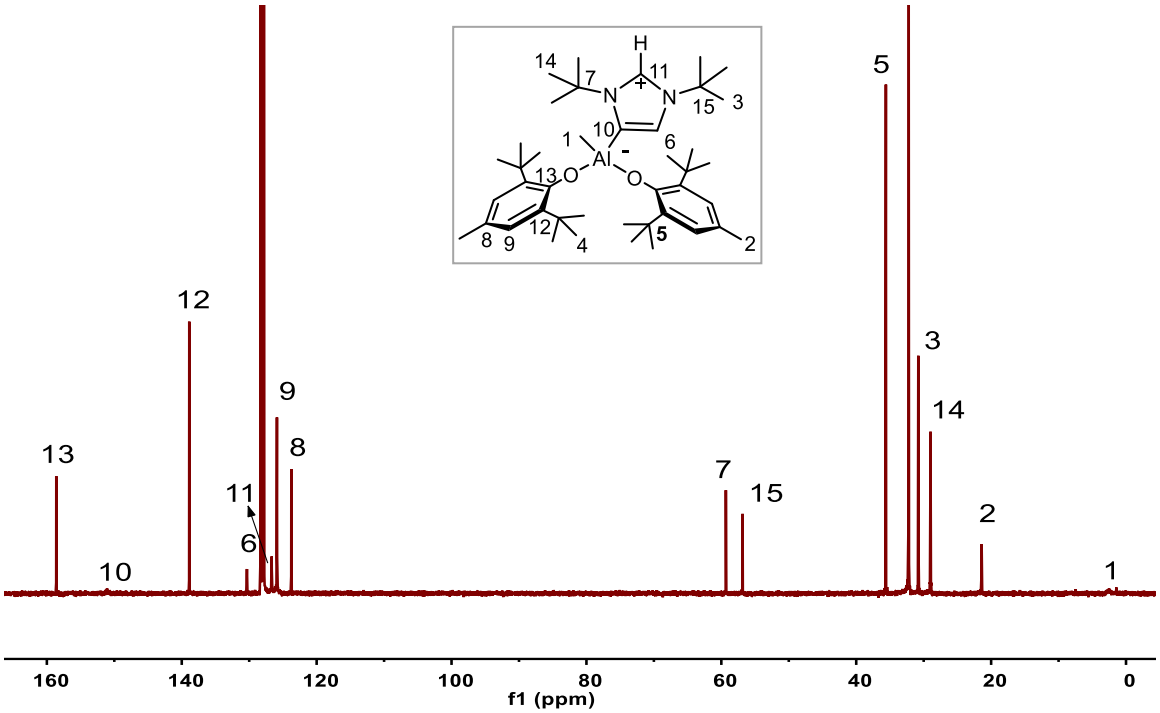

Figure S3. ^{13}C NMR spectrum of the **ALA-1** formed by the stoichiometric reaction of I^{t}Bu and MeAl(BHT)$_2$ (benzene-d_6, RT).

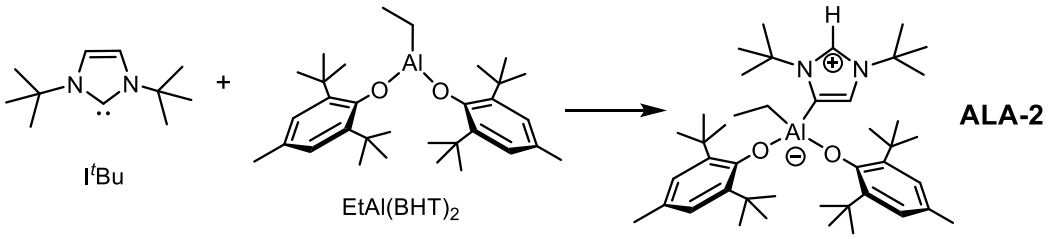

ALA-2: ^{1}H NMR (400 MHz, benzene-d_6, RT): δ 7.17 (s, 4H, Ar–*H*), 7.15 (s, 1H, –C$^+$*H*), 6.88 (s, 1H, N–C*H*=), 2.37 (s, 6H, Ar–CH_3), 1.76 (t, $^3J_{HH}$ = 8 Hz, 3H, Al–CH$_2$CH_3), 1.55 (s, 36H, Ar–C(CH_3)$_3$), 1.42 and 0.74 (s, 18H, N–C(CH_3)$_3$), 1.01 (q, $^3J_{HH}$ = 8 Hz, 2H, Al–CH_2CH$_3$). ^{13}C NMR (100 MHz, benzene-d_6, RT): δ 158.9, 139.0, 126.0, 123.8 (aromatic ring), 151.0 (Al–*C*=), 130.8 (N–*C*H=), 126.6 (–*C*$^+$), 59.2 and 56. 9 (N–*C*(CH$_3$)$_3$), 35.7 (Ar–*C*(CH$_3$)$_3$), 32.4 (Ar–C(*C*H$_3$)$_3$), 30.9 and 29.0 (N–C(*C*H$_3$)$_3$), 21.3 (Ar–*C*H$_3$), 12.0 (Al–CH$_2$*C*H$_3$), 8.4 (Al–*C*H$_2$CH$_3$).

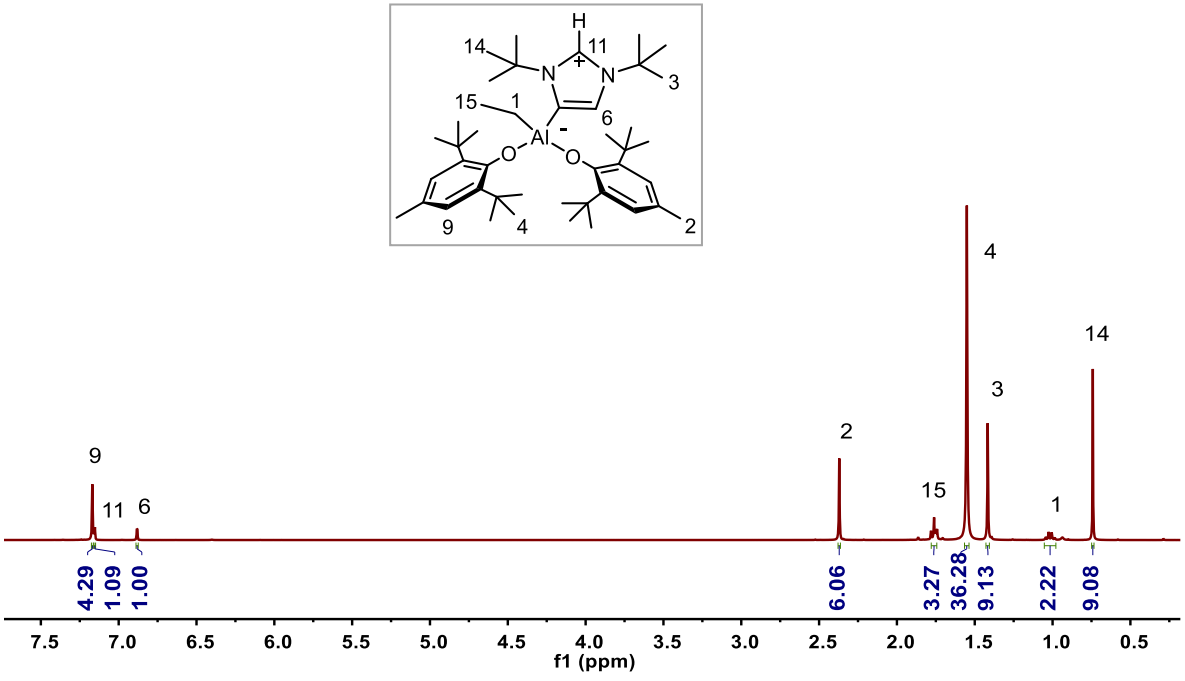

Figure S4. ^{1}H NMR spectrum of the **ALA-2** formed by the stoichiometric reaction of I^{t}Bu and EtAl(BHT)$_2$ (benzene-d_6, RT).

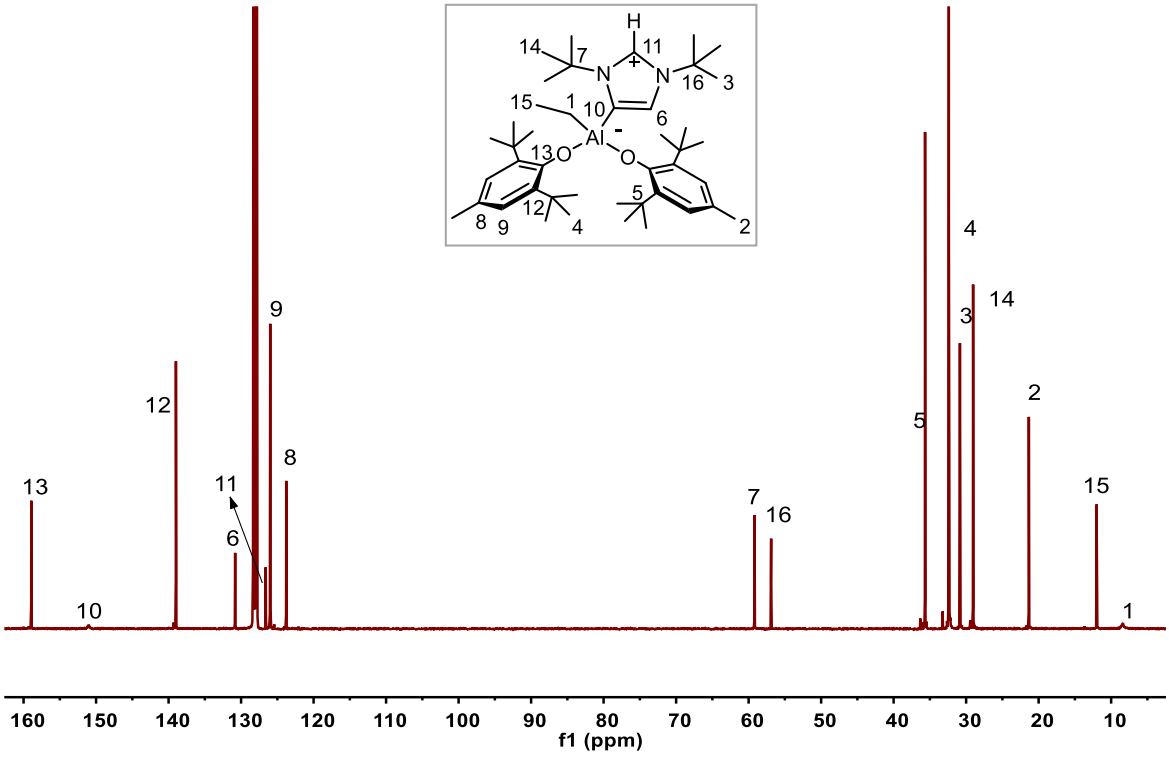

Figure S5. ^{13}C NMR spectrum of the **ALA-2** formed by the stoichiometric reaction of I^{t}Bu and EtAl(BHT)$_2$ (benzene-d_6, RT).

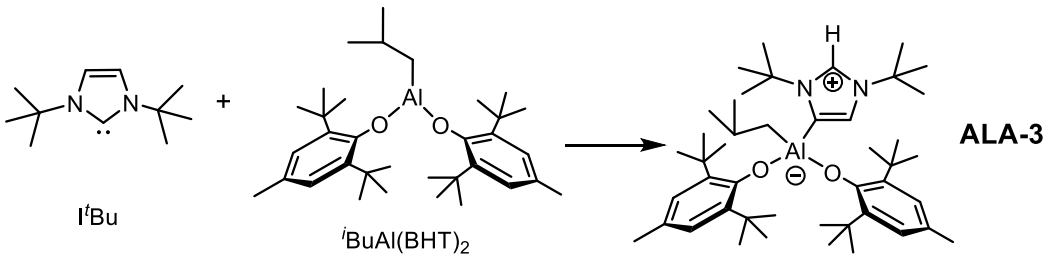

ALA-3: ^{1}H NMR (400 MHz, benzene-d_6, RT): δ 7.16 (s, 1H, –C$^+$*H*), 7.15 (s, 4H, Ar–*H*), 6.92 (s, 1H, N–C*H*=), 2.68 (m, 1H, Al–CH$_2$C*H*(CH$_3$)$_2$), 2.36 (s, 6H, Ar–C*H*$_3$), 1.54 (s, 36H, Ar–C(C*H*$_3$)$_3$), 1.46 (d, $^3J_{HH}$ = 8 Hz, 6H, Al–CH$_2$CH(C*H*$_3$)$_2$), 1.38 and 0.81 (s, 18H, N–C(C*H*$_3$)$_3$), 1.03 (d, $^3J_{HH}$ = 8 Hz, 2H, Al–C*H*$_2$CH(CH$_3$)$_2$). ^{13}C NMR (100 MHz, benzene-d_6, RT): δ 158.9, 139.0, 126.0, 123.8 (aromatic ring), 151.8 (Al–*C*=), 131.1 (N–*C*H=), 126.7 (–*C*$^+$), 59.3 and 57.0 (N–*C*(CH$_3$)$_3$), 35.9 (Ar–*C*(CH$_3$)$_3$), 32.6 (Ar–C(*C*H$_3$)$_3$), 32.1 (Al–CH$_2$*C*H(CH$_3$)$_2$), 31.1 and 29.3 (N–C(*C*H$_3$)$_3$), 29.6 (Al–CH$_2$CH(*C*H$_3$)$_2$), 26. 9 (Al–*C*H$_2$CH(CH$_3$)$_2$), 21.3 (Ar–*C*H$_3$).

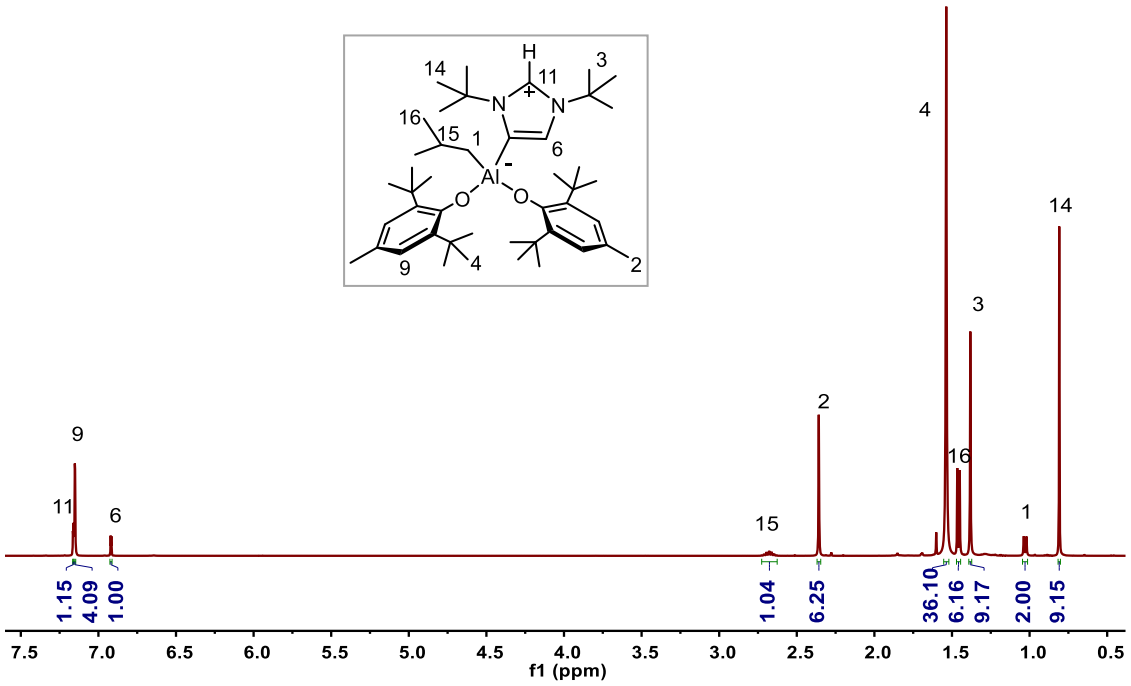

Figure S6. ^{1}H NMR spectrum of the **ALA-3** formed by the stoichiometric reaction of I^{t}Bu and ^{i}BuAl(BHT)$_2$ (benzene-d_6, RT).

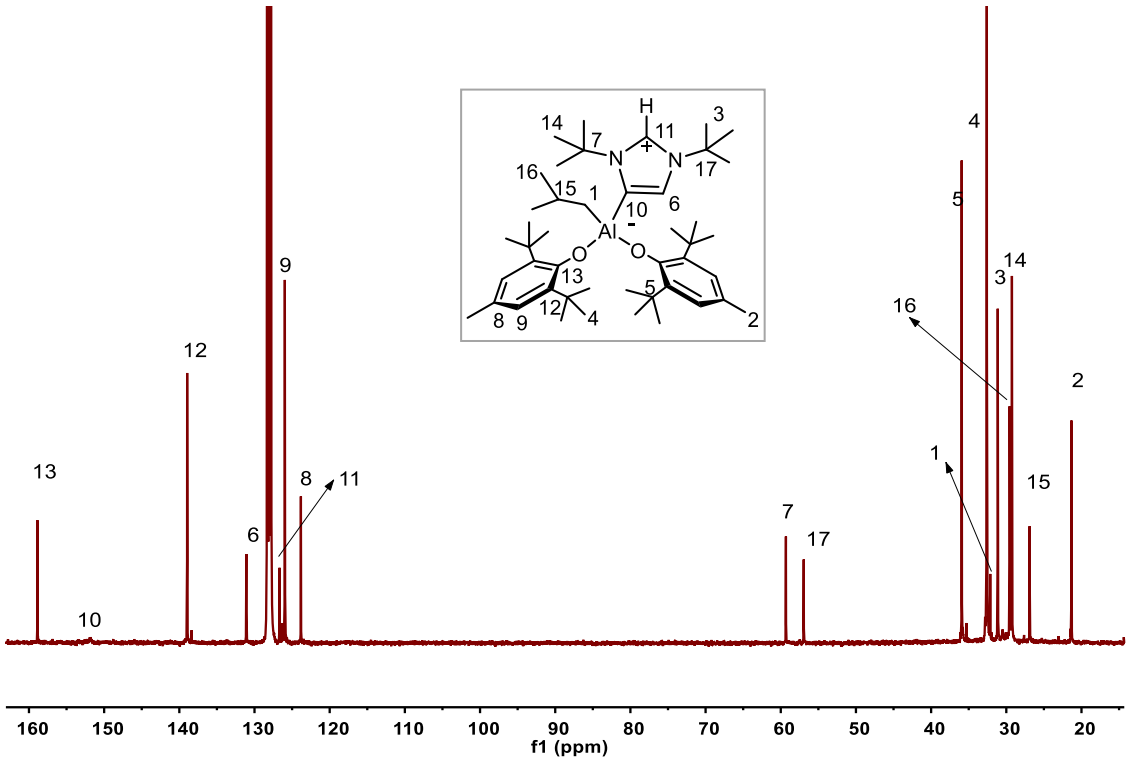

Figure S7. ^{13}C NMR spectrum of the **ALA-3** formed by the stoichiometric reaction of I^{t}Bu and ^{i}BuAl(BHT)$_2$ (benzene-d_6, RT).

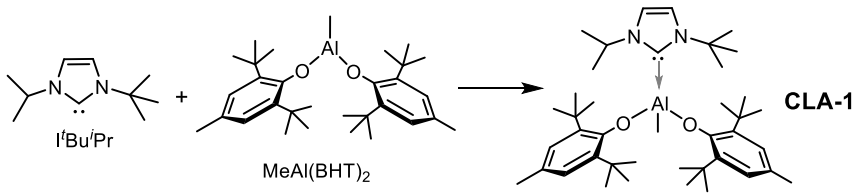

CLA-1: ^{1}H NMR (400 MHz, benzene-d_6, RT): δ 7.15 (s, 4H, Ar–*H*), 6.35 (d, $^3J_{HH}$ = 1.84 Hz, 1H, –*H*C=CH–), 6.13 (d, $^3J_{HH}$ = 1.84 Hz, 1H, –HC=C*H*–), 5.03 (m, 1H, –C*H*(CH$_3$)$_2$), 2.36 (s, 6H, Ar–C*H*$_3$), 1.56 (s, 36H, Ar–C(C*H*$_3$)$_3$), 1.26 (s, 9H, –C(C*H*$_3$)$_3$), 0.77 (m, 6H, –CH(C*H*$_3$)$_2$), 0.38 (s, 3H, Al–C*H*$_3$). ^{13}C NMR (100 MHz, benzene-d_6, RT): δ 168.4 (–*C*$^+$), 156.9, 139.1, 126.4, 124.8 (aromatic ring), 120.7 and 116.3 (–H*C*=*C*H–), 59.5 (–*C*(CH$_3$)$_3$), 51.7 (–*C*H(CH$_3$)$_2$), 36.0 (Ar–*C*(CH$_3$)$_3$), 32.8 (Ar–C(*C*H$_3$)$_3$), 31.5 (N–C(*C*H$_3$)$_3$), 24.0 (–CH(*C*H$_3$)$_2$), 21.3 (Ar–*C*H$_3$), 5.4 (Al–*C*H$_3$).

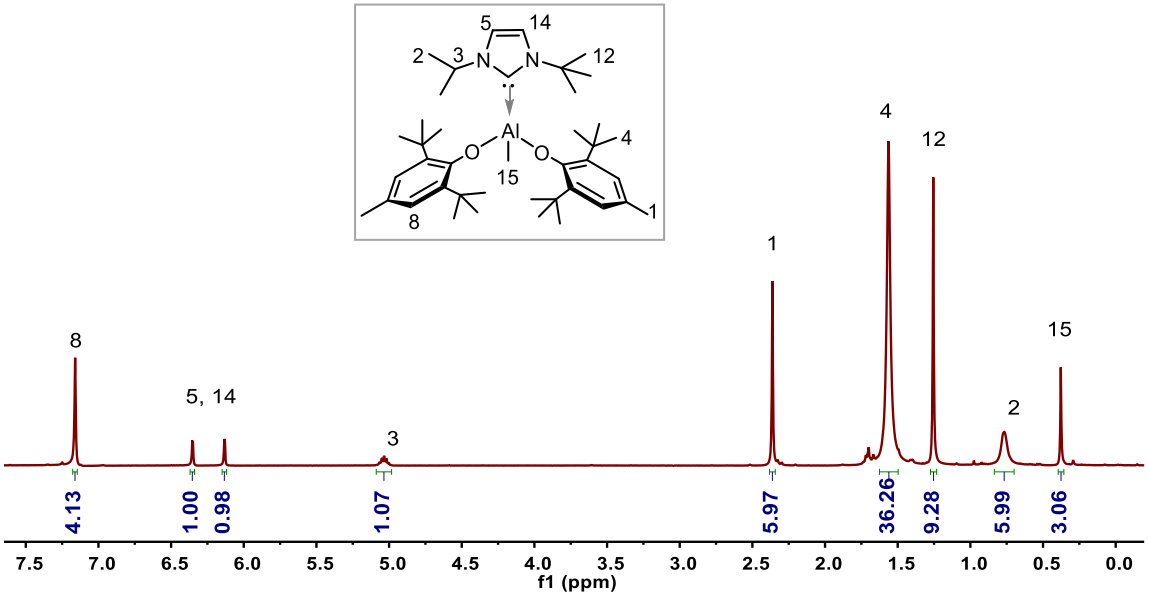

Figure S8. ^{1}H NMR spectrum of the **CLA-1** formed by the stoichiometric reaction of I^{t}Bu^{i}Pr and MeAl(BHT)$_2$ (benzene-d_6, RT).

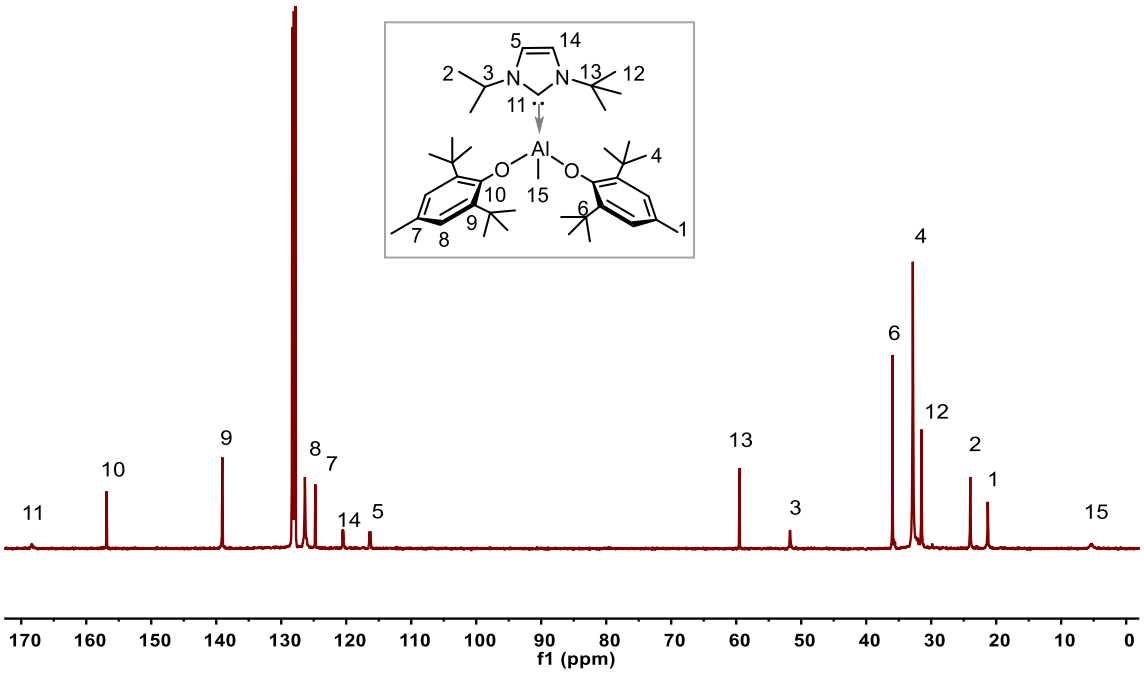

Figure S9. ^{13}C NMR spectrum of the **CLA-1** formed by the stoichiometric reaction of I^{t}Bu^{i}Pr and MeAl(BHT)$_2$ (benzene-d_6, RT).

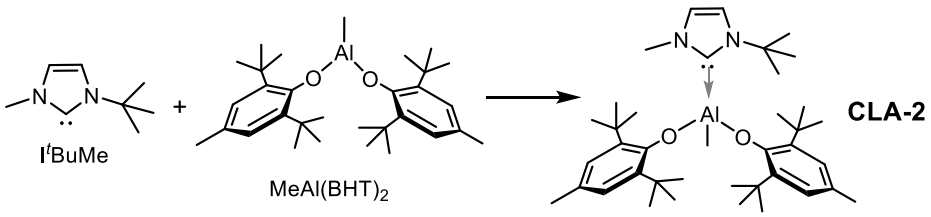

CLA-2: ^{1}H NMR (400 MHz, benzene-d_6, RT): δ 7.15 (s, 4H, Ar–*H*), 6.20 (d, $^3J_{HH}$ = 2.04 Hz, 1H, –*H*C=CH–), 5.65 (d, $^3J_{HH}$ = 2.04 Hz, 1H, –HC=C*H*–), 3.31 (s, 3H, NCH_3), 2.33 (s, 6H, Ar–CH_3), 1.47 (s, 36H, Ar–C(CH_3)$_3$), 1.27 (s, 9H, –C(CH_3)$_3$), 0.33 (s, 3H, Al–CH_3). ^{13}C NMR (100 MHz, benzene-d_6, RT): δ 169.7 (–*C*$^+$), 156.8, 138.9, 126.4, 124.8 (aromatic ring), 121.9 and 119.3 (–HC=*C*H–), 59.6 (–*C*(CH$_3$)$_3$), 39.0 (N*C*H$_3$), 35.7 (Ar–*C*(CH$_3$)$_3$), 31.2 (Ar–C(*C*H$_3$)$_3$), 21.4 (Ar–*C*H$_3$), 4.2 (Al–*C*H$_3$).

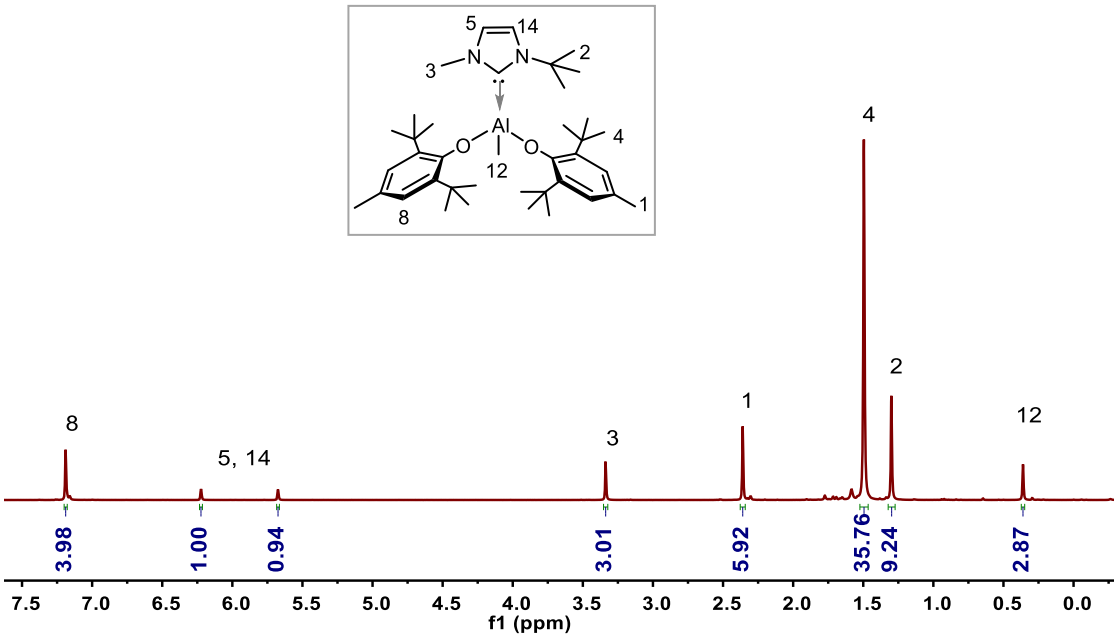

Figure S10. ^{1}H NMR spectrum of the **CLA-2** formed by the stoichiometric reaction of I^{t}BuMe and MeAl(BHT)$_2$ (benzene-d_6, RT).

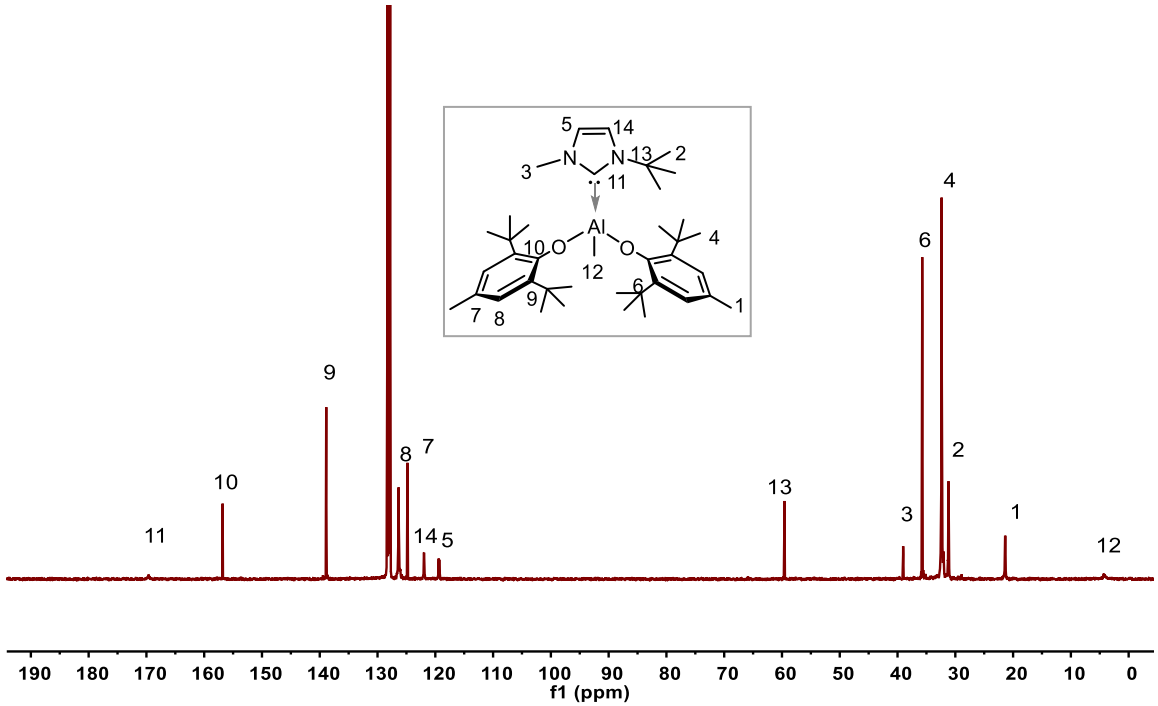

Figure S11. ^{13}C NMR spectrum of the **CLA-2** formed by the stoichiometric reaction of I^{t}BuMe and MeAl(BHT)$_2$ (benzene-d_6, RT).

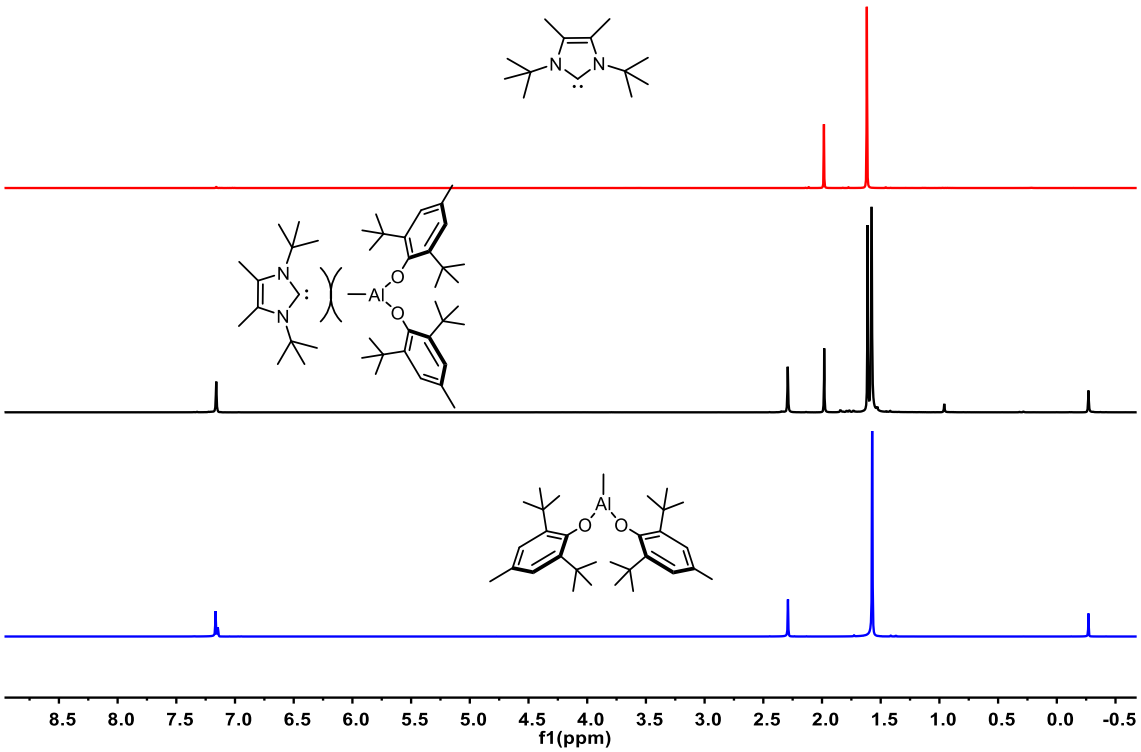

Figure S12. Overlay of ^{1}H NMR spectra for Me-I^{t}Bu, MeAl(BHT)$_2$ and equivalent mixture of Me-I^{t}Bu and MeAl(BHT)$_2$ (benzene-d_6, RT).

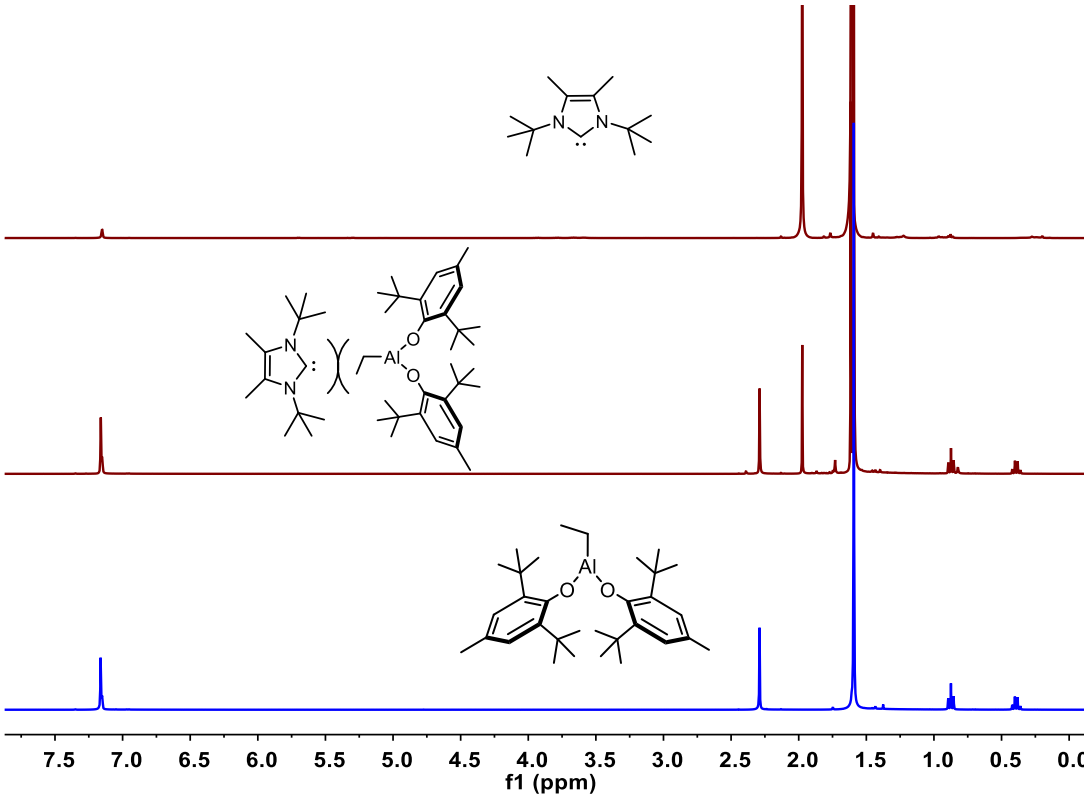

Figure S13. Overlay of ^{1}H NMR spectra for Me-I^{t}Bu, EtAl(BHT)$_2$ and equivalent mixture of Me-I^{t}Bu

and EtAl(BHT)$_2$ (benzene-d_6, RT).

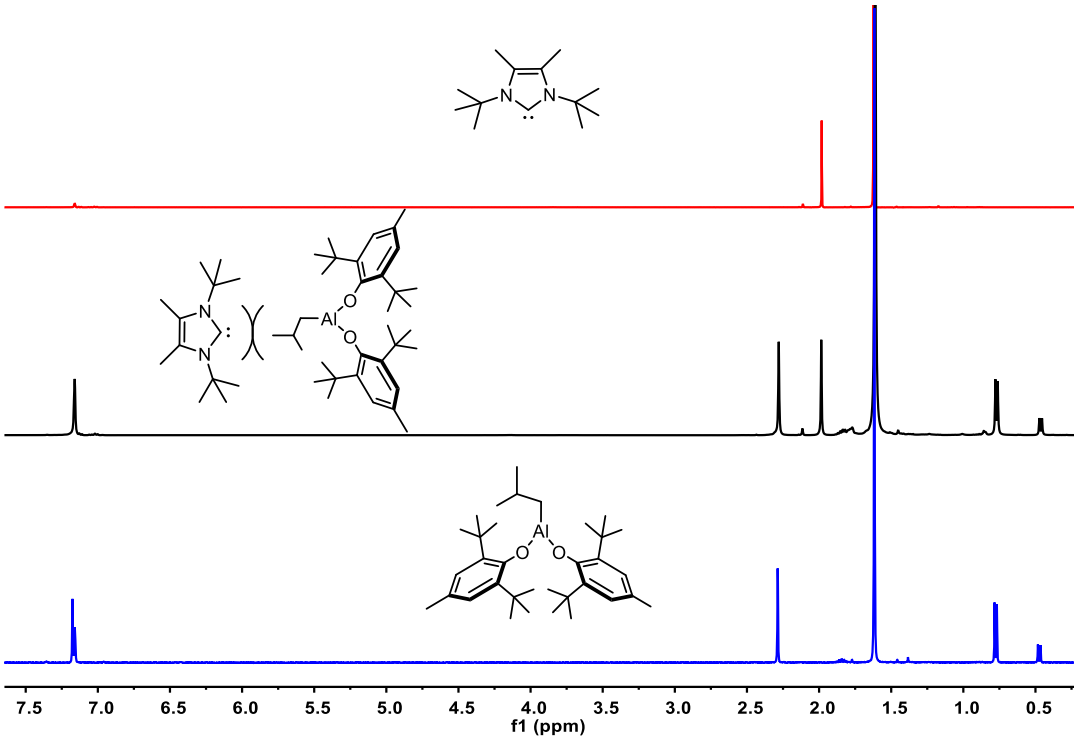

Figure S14. Overlay of ^{1}H NMR spectra for Me-I^{t}Bu, ^{i}BuAl(BHT)$_2$ and equivalent mixture of Me-I^{t}Bu and ^{i}BuAl(BHT)$_2$ (benzene-d_6, RT).

General Polymerization Procedures.

The polymerizations were performed in either 20 mL glass reactors inside the glovebox for RT runs or 25 mL flame-dried Schlenk tubes interfaced to the dual-manifold Schlenk line for the runs using an external temperature bath. For the polymerizations at RT, a predetermined amount of LA was first dissolved in solvent containing predetermined amount of monomer inside a glovebox. The mixture was stirred for 10 minutes, and then the polymerization was triggered by rapid addition of a predetermined amount of LB solution via a dry syringe under vigorous stirring. Take Table 1, run 1 as an example, MeAl(BHT)$_2$ (24 μmol, 11.8 mg) and β-AL (2.4 mmol, 0.25 g) were dissolved in CH_2Cl_2 (2.7 mL), and the mixture was stirred for 10 minutes. Then the polymerization was triggered by rapid addition of solution of LB (12 μmol, 2.2 mg) in 1 mL of CH_2Cl_2 via a dry syringe under vigorous stirring. After the

measured time interval, a 0.2 mL aliquot was taken from the reaction mixture via syringe and quickly quenched into a 2 mL septum-sealed vial containing 0.4 mL of $CDCl_3$ with by 250 ppm of benzoic acid; the quenched aliquots were later analyzed by ^{1}H NMR to obtain the percent monomer conversion data. For the polymerizations under an external temperature bath, the Schlenk tube was charged with a predetermined amount of LA, monomer and solvent, sealed, taken out of glovebox, and then immersed in the external temperature bath for 10 min. The polymerization was started by the rapid addition of an LB solution via a gastight syringe to the above-mentioned mixture under vigorous stirring. After a desired period of time, the polymerization was immediately quenched by addition of 5 mL of ethanol acidified with HCl (5%); the quenched mixture was precipitated into 100 mL of ethanol, filtered, washed with ethanol to remove any unreacted monomer, and dried in a vacuum oven at RT to a constant weight.

Characterizations.

NMR spectra were recorded on a Varian 400 MHz spectrometer. Chemical shifts for ^{1}H NMR and ^{13}C NMR spectra were referenced to internal solvent resonances and were reported as parts per million relative to $SiMe_4$. Absolute weight-average molecular weight (M_w), number average molecular weight (M_n), and molecular weight distributions ($Đ = M_w/M_n$) of polymer samples were measured by gel permeation chromatography (GPC) at a flow rate of 1.0 mL/min with DCM or DMF as the eluent on a Waters E2695 GPC instrument equipped with a Wyatt OPTILAB® T-Rex refractive-index detector, a Wyatt DAWN HELEOS II multi (18)-angle light scattering detector, one Agilent Plgel 5 μm guard column, and two Agilent Plgel 5 μm Mixed-C columns. The resultant chromatograms were processed with a Wyatt ASTRA 7 software. The refractive index increment (dn/dc) of polymer was determined by a Wyatt OPTILAB® T-rEx refractive-index detector and calculated using ASTRA software. dn/dc

values for PAL, PMS, and PMC are 0.0787 (DMF)[7], 0.0774 (DCM), and 0.0487 (DCM). Glass-transition temperatures (T_g) were measured by differential scanning calorimetry (DSC) on a DSC2500, TA Instrument, under N_2 atmosphere. All T_g values were obtained from the second scan after the thermal history was removed from the first scan. The first heating rate was 10 °C/min, while the cooling rate was 5 °C/min and the second heating rate was 10 °C/min. The onset decomposition temperatures (T_d, defined at 5% weight loss) of the polymers were measured by thermal gravimetric analysis (TGA) on a TGA550, TA Instrument. Polymer samples were heated from ambient temperatures to 700 °C at a rate of 20 °C/min under N_2 atmosphere. Fourier transform infrared (FT-IR) spectroscopy was performed on a BRUKER TENSOR 27 FT-IR spectrometer equipped with platinum ATR at room temperature in the range of 550–4000 cm^{-1}.

The isolated low molecular weight samples were analyzed by matrix assisted laser desorption/ionization time-of-flight mass spectroscopy (MALDI–TOF MS); the experiment was performed on a Bruker Reflex II mass spectrometer operated in positive ion, reflector mode using a Nd:YAG laser at 355 nm and 25 kV accelerating voltage. A thin layer of a 1% NaI solution was first deposited on the target plate, followed by 0.6 μl of both sample and matrix (dithranol, 20 mg/mL in methanol, 10% AAC). External calibration was done using a peptide calibration mixture (4 to 6 peptides) on a spot adjacent to the sample.

Single crystals suitable for single-crystal X-ray analysis were grown from a mixture solution of benzene and hexane. The crystals were mounted on a thin glass fiber, quickly covered with a layer of Paratone-N oil (Exxon, dried and degassed at 120 °C/10^{-6} Torr for 24 h), and then transferred into the cold nitrogen stream of a BRUKER D8 VENTURE diffractometer using Mo Kα radiation (λ = 0.71073 Å) at 193 K for data collections. The structures were refined by full-matrix least-squares on F2 for all

reflections. All non-hydrogen atoms were refined with anisotropic displacement parameters, whereas hydrogen atoms were included in the structure factor calculations at idealized positions. Crystallographic data have been deposited with the Cambridge Crystallographic Data Center as supplementary publications (Deposition Numbers: 2239989, 2239990, 2239991, 2239993 for **ALA-1**, **ALA-2**, **ALA-3**, **CLA-1**, respectively). These data can be obtained free of charge from The Cambridge Crystallographic Data Centre via www.ccdc.cam.ac.uk/ data_request/cif.

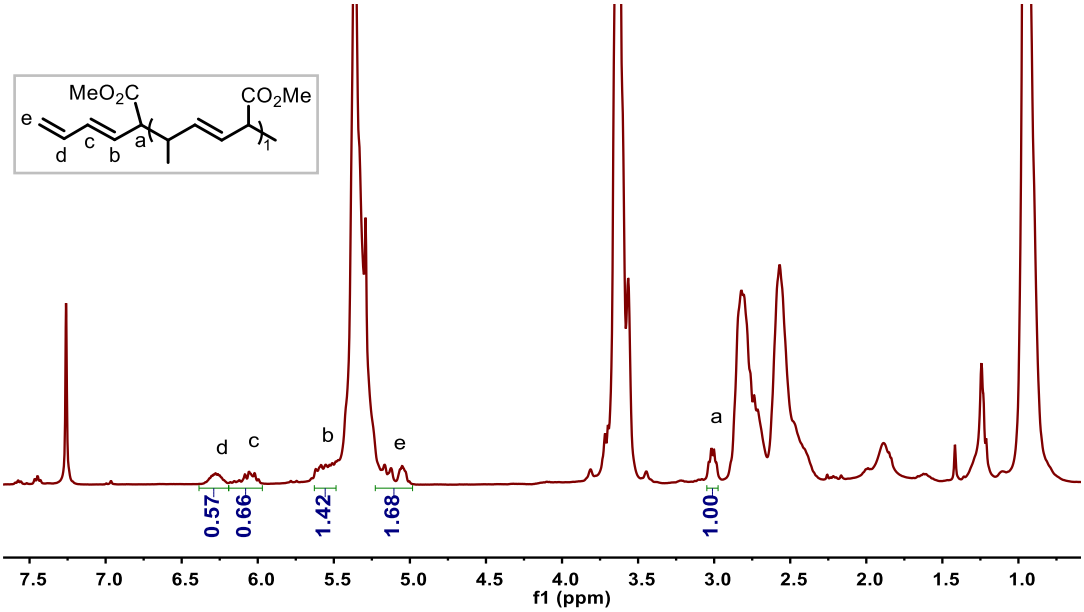

Figure S15. ^{1}H NMR spectrum ($CDCl_3$) of low-MW PMS (condition: $[MS]_0$:$[MeAl(BHT)_2]_0$:$[Me\text{-}I^tBu]_0$ = 400:3:1, $[MS]_0$ = 1 M in toluene, RT, 2 min).

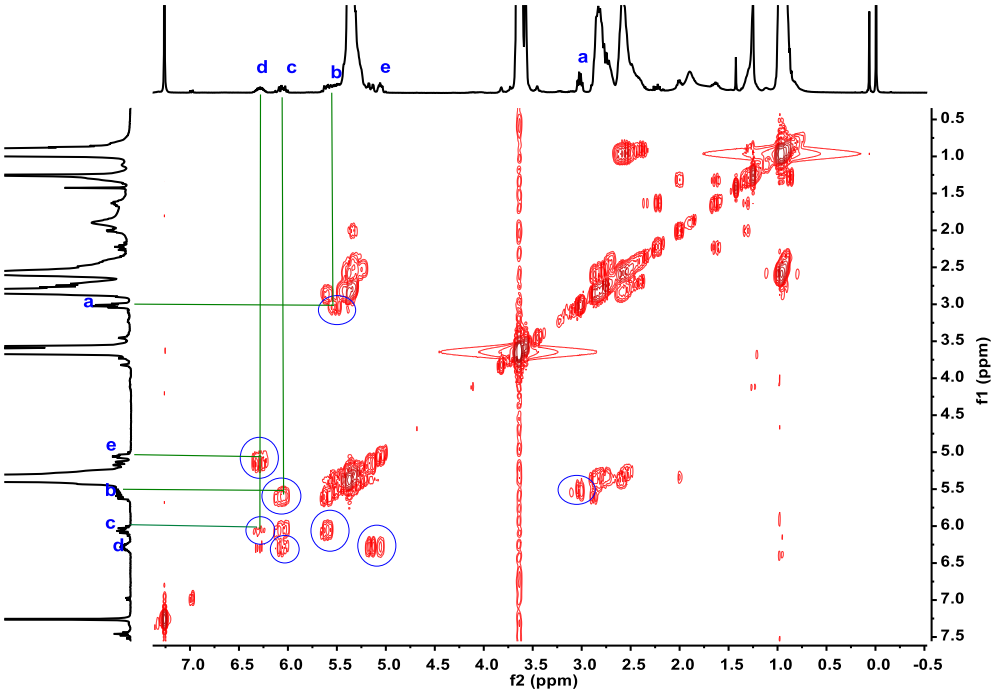

Figure S16. ^{1}H-^{1}H COSY spectra of low-MW PMS ($CDCl_3$).

Synthesis and characterization of polymerization active species.

A 0.4 mL toluene solution of Me-I^{t}Bu (16.6 mg, 0.08 mmol) was added dropwise via syringe to a 0.4 mL toluene solution of MS (10.1 mg, 0.08 mmol) and $MeAl(BHT)_2$ (38.4 mg, 0.08 mmol). After 5 min, the solvent was removed, yielding contacted [Me-I^{t}Bu]$^{+}$/enolaluminate ion pair as the clean product. ^{1}H NMR (400 MHz, CD_2Cl_2, 25 °C): δ 7.95 (s, 1H, –C^{+}*H*), 2.41 (s, 6H, C*H*$_3$–C=C), 1.69 (s, 18H, NC(C*H*$_3$)$_3$), 6.95 and 6.48 (dd, $^{3}J_{HH}$ = 15.1 and 14.8 Hz, 11.0 and 11.3 Hz, 1H, CH_2=CHCH=C*H*CH=), 6.89 (s, 4H, Ar–H), 6.38-6.19 (m, 1H, CH_2=C*H*CH=CHCH=); 5.65 and 5.44 (dd, $^{3}J_{HH}$ = 15.1 and 14.7 Hz, 10.7 and 10.9 Hz, 1H, CH_2=CHC*H*=CHCH=), 4.72 and 4.63 (dd, $^{3}J_{HH}$ = 10.9 Hz, 2.3 Hz, 1H, C*H*$_2$=CHCH=CHCH=), 4.50 and 4.45 (dd, $^{3}J_{HH}$ = 10 Hz, 2.3 Hz, 1H, C*H*$_2$=CHCH=CHCH=); 4.35 and 4.17 (d, $^{3}J_{HH}$ = 11.3 Hz and 10.8 Hz, 1H, CH_2=CHCH=CHC*H*=); 3.51 and 3.35 (s, 3H, –OC*H*$_3$); 2.19 (s, 6H, Ar–C*H*$_3$); 1.41-1.37 (s, 36H, Ar–C(C*H*$_3$)$_3$); -0.62 and -0.67 (s, 3H, Al–C*H*$_3$). ^{13}C NMR (100 MHz, CD_2Cl_2, 25 °C): δ 128.8 (–*C*$^{+}$H); 122.9 (CH_3*C*=*C*CH_3); 62.1

($NC(CH_3)_3$); 29.9 ($NC(CH_3)_3$); 12.1($CH_3C{=}CCH_3$); 165.5 and 161.9 (=*C*–O–Al); 156.8, 139.4, 130.2, 125.8 (aromatic ring), 140.9 and 140.7 ($CH_2{=}CHCH{=}CHCH{=}$); 137.2 and 135.3 ($CH_2{=}CHCH{=}CHCH{=}$); 116.9 and 116.6 ($CH_2{=}CHCH{=}CHCH{=}$); 105.6 ($CH_2{=}CHCH{=}CHCH{=}$); 82.0 and 74.4 ($CH_2{=}CHCH{=}CHCH{=}$); 54.2 and 53.6 ($-OCH_3$); 35.5 (Ar–$C(CH_3)_3$); 31.9 (Ar–$C(CH_3)_3$); 21.3 (Ar–CH_3); -4.1 (Al-CH_3).

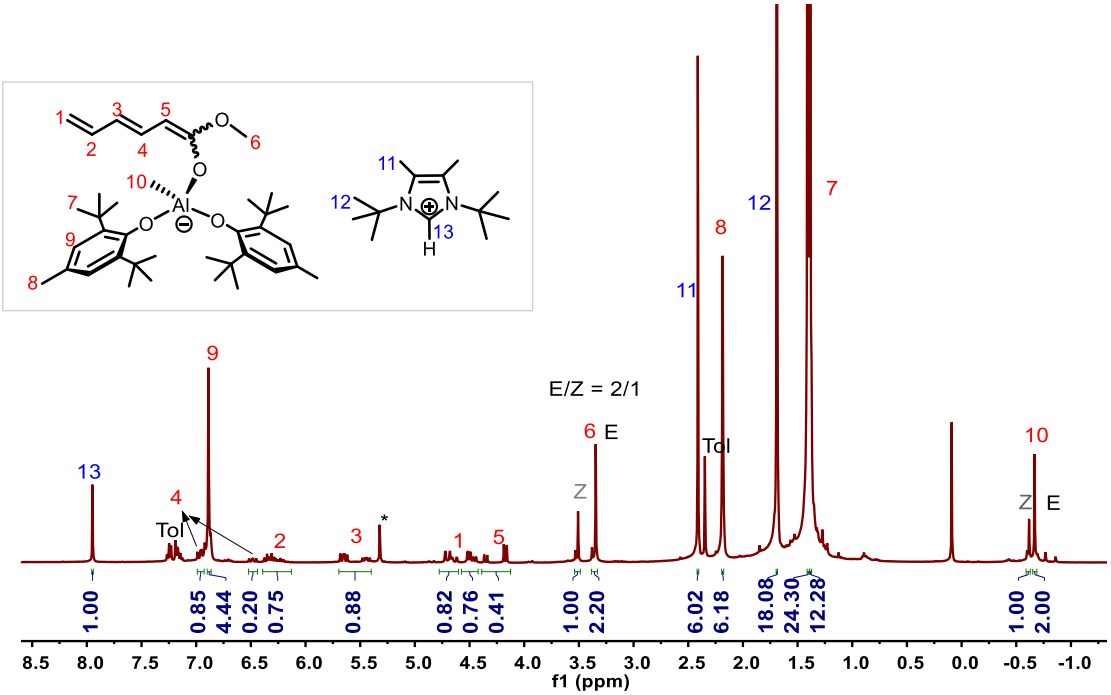

Figure S17. ^{1}H NMR spectrum of ion pair active species in the stoichiometric reaction (CD_2Cl_2, RT).

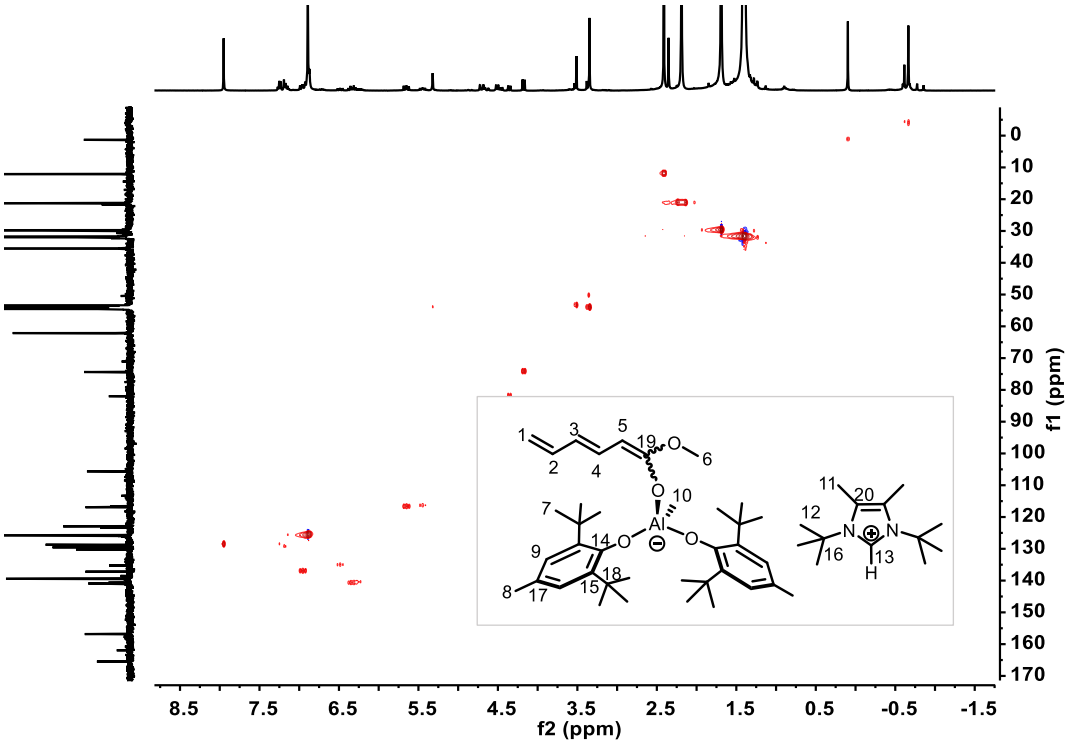

Figure S18. ^{1}H-^{13}C correlation NMR spectrum of ion pair active species in the stoichiometric reaction (CD_2Cl_2, RT).

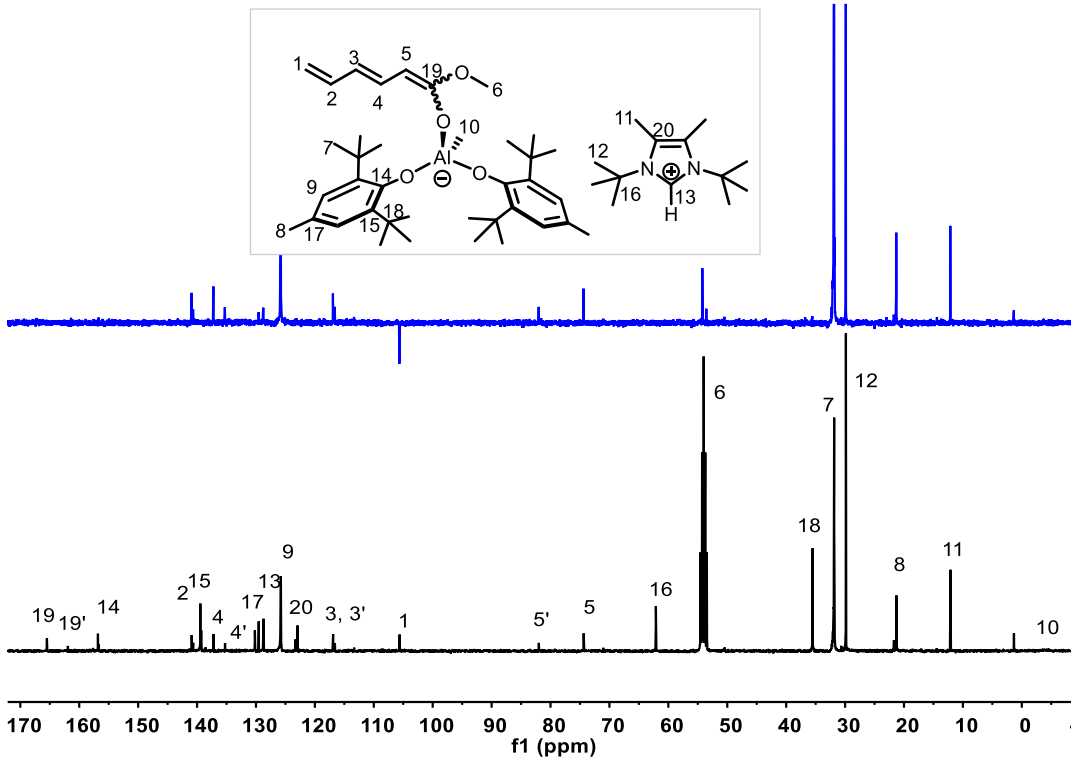

Figure S19. DEPT-135 (top) and ^{13}C NMR spectra (bottom) of ion pair active species in the stoichiometric reaction (CD_2Cl_2, RT).

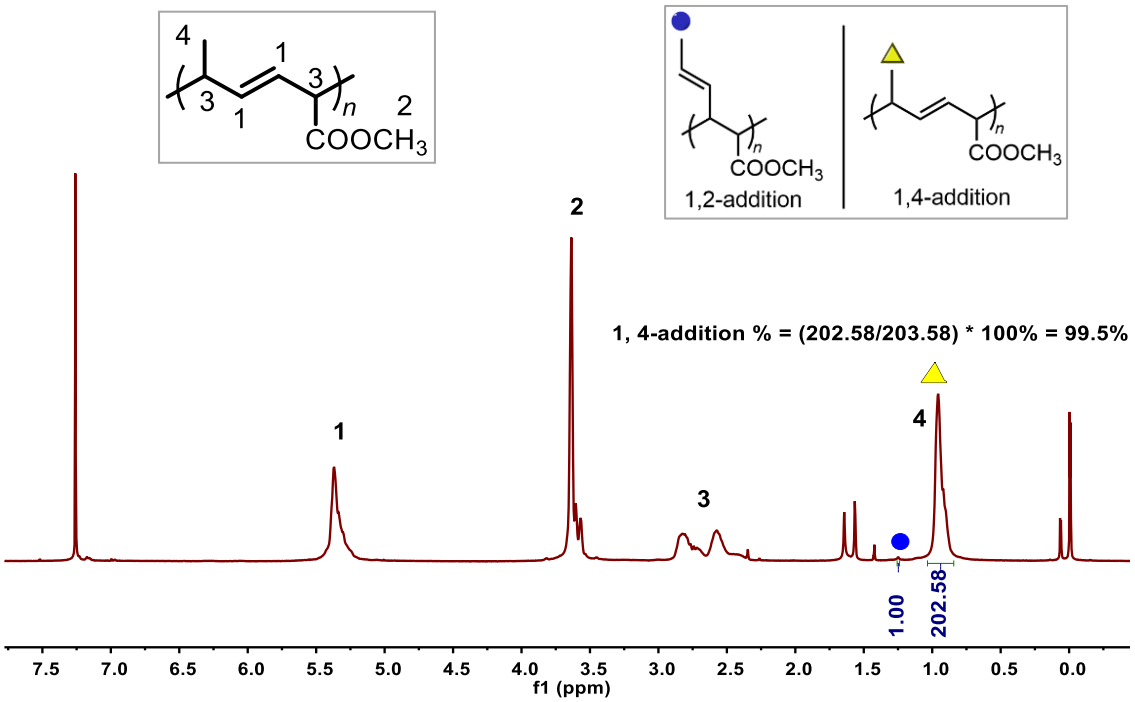

Figure S20. ^{1}H NMR spectrum (CD_3Cl, RT) of representative PMS sample produced by $MeAl(BHT)_2$/Me-I^{t}Bu FLP.

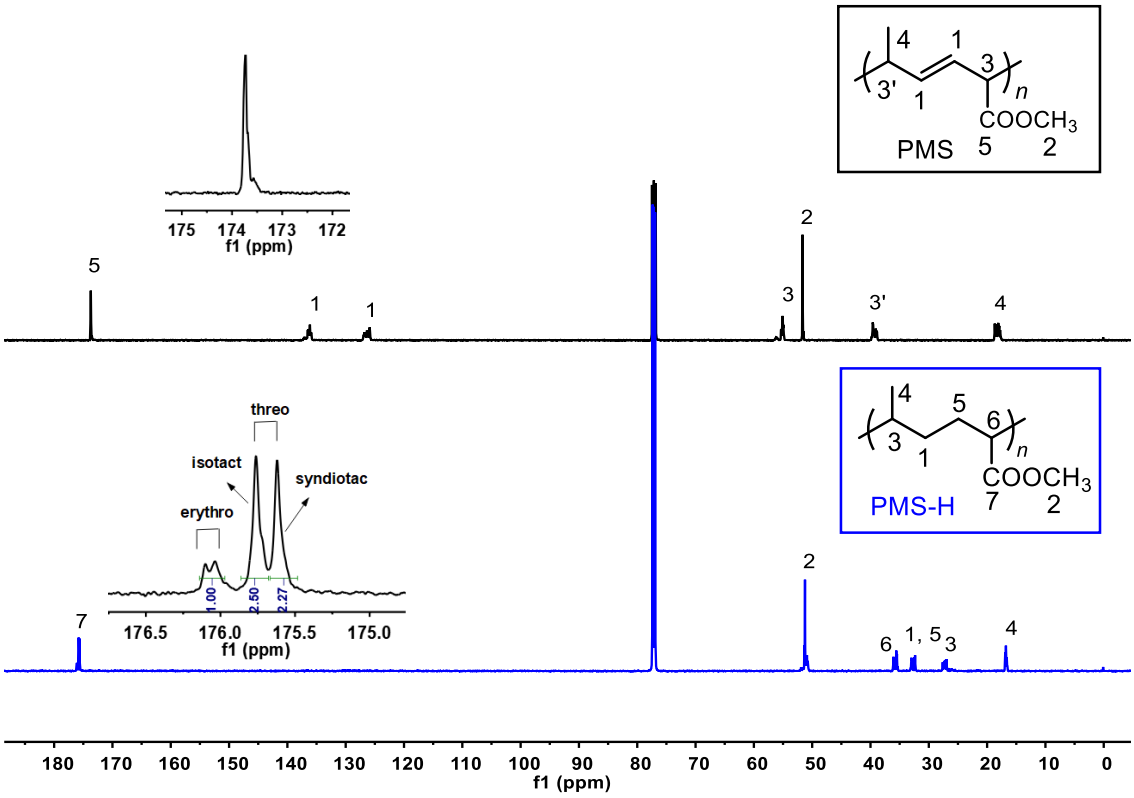

Figure S21. ^{13}C NMR spectra (CD_3Cl, RT) of PMS (top) and PMS-H (bottom).

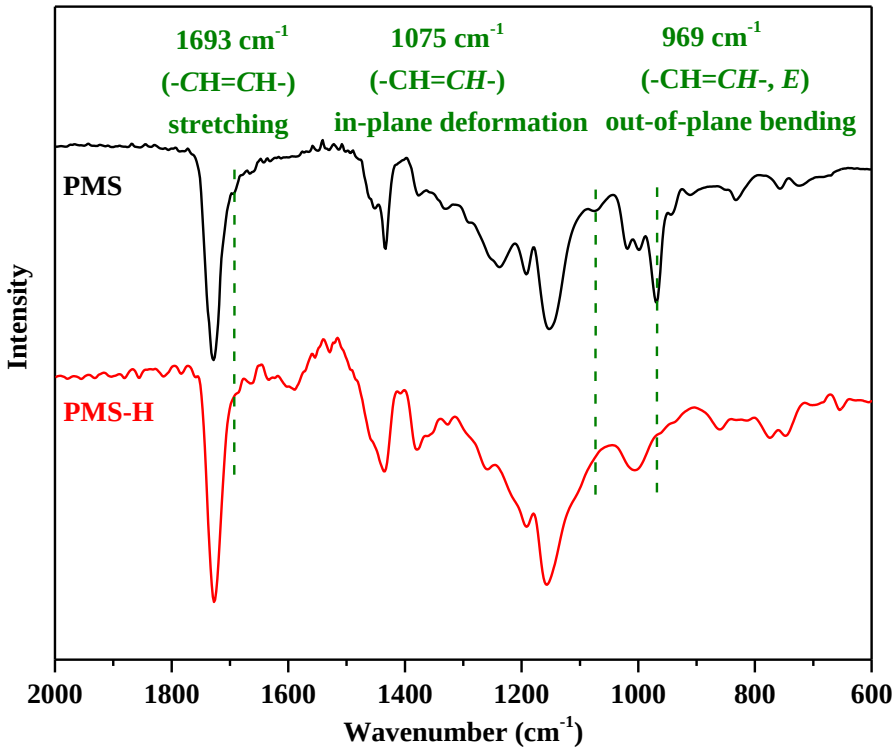

Figure S22. FT-IR spectra of PMS (black) and PMS-H (red).

References

1. X.-J. Wang and M. Hong, *Angew. Chem. Int. Ed.*, 2020, **59**, 2664-2668.
2. S. J. Ryan, S. D. Schimler, D. C. Bland and M. S. Sanford, *Org. Lett.*, 2015, **17**, 1866-1869.
3. P. Rios, H. Fouilloux, P. Vidossich, J. Diez, A. Lledos and S. Conejero, *Angew. Chem. Int. Ed.*, 2018, **57**, 3217-3221.
4. A. Levens, F. An, M. Breugst, H. Mayr and D. W. Lupton, *Org. Lett.*, 2016, **18**, 3566-3569.
5. A. A. Grishina, S. M. Polyakova, R. A. Kunetskiy, I. Cisarova and I. M. Lyapkalo, *Chem. Eur. J.*, 2011, **17**, 96-100.
6. A. P. Shreve, R. Mulhaupt, W. Fultz, J. Calabrese, W. Robbins and S. D. Ittel, *Organometallics*, 1988, **7**, 409-416.
7. X.-J. Wang and M. Hong, *Angew. Chem. Int. Ed.*, 2020, **59**, 2664-2668.